Title

THE SURFACE DIFFUSION OF HIGH TEMPERATURE VAPORS IN POROUS ALUMINA

Authors

Jacobson, N.S.
Opila, E.J.
Searcy, A.W.

Publication Date

1983-08-01

LBL-16491 c. 2
Preprint

Lawrence Berkeley Laboratory
UNIVERSITY OF CALIFORNIA

Materials & Molecular Research Division

Submitted to High Temperature Science

THE SURFACE DIFFUSION OF HIGH TEMPERATURE VAPORS IN POROUS ALUMINA

N.S. Jacobson, E.J. Opila, and A.W. Searcy

August 1983

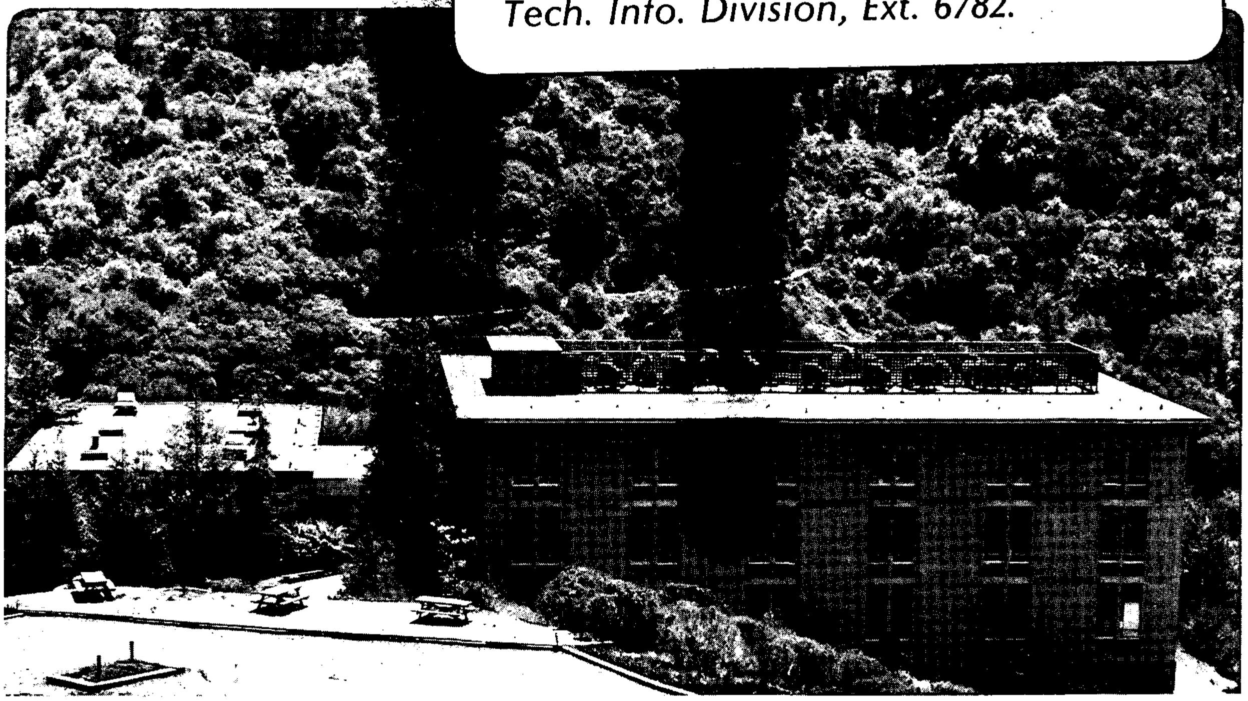

LBL-16491 c.2

Prepared for the U.S. Department of Energy under Contract DE-AC03-76SF00098

LBL-16491

THE SURFACE DIFFUSION OF HIGH TEMPERATURE VAPORS IN POROUS ALUMINA

Nathan S. Jacobson[1], Elizabeth J. Opila[2], and
Alan W. Searcy

Materials and Molecular Research Division
Lawrence Berkeley Laboratory
and
Department of Materials Science and Mineral Engineering
University of California
Berkeley, California 94720

August 1983

---

[1] Present address: NASA-Lewis Research Center, Cleveland, Ohio

[2] Present address: Monolithic Memories, Inc., Sunnyvale, California

This work was supported by the Division of Materials Science, Office of Basic Energy Science, U.S. Department of Energy under Contract Number DE-AC03-76SF00098.

Abstract

In porous alumina barriers ∿1 mm thick, 45% porosity, and ∿1.2 μm average pore diameter, transmission coefficients for NaCl, NaF, and LiF vapors are ∿2.6, 6, and 12 times that of He, indicating that surface diffusion contributes to the transmission. For Zn vapor, transmission coefficients are 1.2 to 3.5 that of He through the ∿1.2 μm pores and 18 times that of He through 0.14 μm pores. The temperature dependences of LiF and NaCl transmission by surface diffusion are close to those for Knudsen effusion, a result which indicates that the activated complex for surface diffusion is very weakly bound to the surface. Above their melting points, the transmission of LiF and NaCl are irreproducible, but are usually markedly increased, perhaps because a liquid-like film partially penetrates the barrier.

Index Entries:

Alumina, porous
Knudsen effusion
Surface diffusion, at high temperatures
Transport, in porous media
Vapors, alkali halide
Vapors, zinc

INTRODUCTION

Equilibrium pressures derived from effusion studies usually assume that Knudsen flow is the only significant path of vapor transport through the orifice [1]. This may not always be the case. Effusion studies are sometimes thwarted by the "creep" or "bulk surface flow" of large amounts of material up the cell walls and out of the orifice [2,3]. In this laboratory [4], this phenomenon has been observed with CrF_3, CoF_2, and FeF_2. It is a matter for concern that less obvious transport by surface diffusion may often contribute to effusion fluxes and introduce errors into vapor pressure measurements.

Winterbottom and Hirth [5-7] drew attention to this possibility and developed a theory for combined surface diffusion of a dilute monolayer of adsorbed vapor molecules and Knudsen flow through short cylindrical or conical orifices. To calculate from the model the surface diffusion contribution to the total flux, the surface diffusion coefficient and the energy of desorption are required. Generally, these data are unavailable. However, Winterbottom and Hirth used data for silver vapor on nickel and molybdenum surfaces to support their theoretical conclusion that the greatest surface diffusion contributions will be found with orifices of small diameters and small length-to-radius ratios or knife-edges. Ward et al. [8,9] have done computer simulations of Knudsen and surface diffusion through orifices and obtained results in general agreement with the model of Winterbottom and Hirth.

There has been little experimental data with which to compare this model. Boyer and Meadowcroft [10] have measured the free energy of vaporization of silver under conditions which Winterbottom and Hirth predict will promote surface diffusion. Use of a molybdenum cell lid with a small diameter knife-edge orifice yields an apparent $\Delta G = 227,600 + 85T$ J/mol. When corrected for surface diffusion, this value becomes much closer to the accepted free energy of $\Delta G = 266,100 + 110T$ J/mol. The difference between the apparent value of ΔG and the accepted value becomes much less for larger orifice diameters. Grimley et al. [11] have observed altered angular distributions for samarium vapor emerging from tantalum and boron nitride orifices, but they attribute this to bulk diffusion in the orifice walls.

The surface diffusion contributions to effusion modeled by Winterbottom and Hirth arise primarily from end effects, so that surface diffusion that obeys their model would be unimportant in long channels or in porous barriers, which can be viewed as a network of long irregularly shaped channels. However, extensive studies with barriers traversed by pores of ∿10 nm cross section at temperatures at or near room temperature show that for such small pores surface diffusion by gases can be a major path of transport [12]. In a typical study, the transmission behavior of a gas under investigation is compared to that of He, for which adsorption and surface diffusion are negligible at room temperature. CO, for example, passes several times faster than He through a graphon plug, which has ∿5 nm pores [12]. The enhancement of CO flow is attributed to diffusion in a dilute monolayer adsorbed on the pore walls. Gilliland et al. [13] found that various hydrocarbons pass through vycor up to 17 times faster than He does. They could not reconcile this result with submonolayer coverage, and instead developed a theory based on a spreading film. At only a few hundred degrees centigrade, kT, where k is the Boltzmann constant and T is the absolute temperature, becomes large relative to the bonding energies of most gases to surfaces. Surface diffusion then becomes unimportant because most gas molecules desorb before they have moved a significant distance from the point of impact with the surface.

Mohazzabi and Searcy [14] have shown that porous barrier studies can provide insights into equilibration of monomer-dimer vapor mixtures in pressure gradients along surfaces. It seemed likely that barrier studies might provide useful information on surface diffusion of high temperature vapors if the bonding energy of the vapor molecules to the surface is large enough to be comparable to kT. To test this possibility, various high temperature vapors are passed through porous alumina. The diffusion rates are compared to Knudsen diffusion rates measured for He. Transmission probabilities are used to describe the diffusion. These are defined as the ratio of J_e, the molar flux of vapor per unit area that escapes from the plug, to J_o, the flux per unit area that strikes the plug. Transmission probabilities near those measured for He indicate that Knudsen flow is the primary mechanism of transport; larger transmission probabilities indicate the presence of an additional path of transport--presumably surface diffusion.

EXPERIMENTAL

Characterization of Porous Alumina. Two types of porous alumina were used--one with an average pore-cross-section of 1.2 ± 0.2 μm and one with an average pore cross section of 0.14 ± 0.02 μm. Both were used as disks 0.95 ± 0.05 mm thick. The alumina of larger pore size was made at the Lawrence Berkeley Laboratory ceramics shop from an alumina greenware (Western Gold and Platinum, Belmont CA). This material was a mixture of ∿1 μm cross section alumina particles (99.5% pure) and a resin binder. The mixture was fired at about 1250°C for about one hour. This process vaporized the resin binder and left a partially sintered porous product, called Alumina I.

The surface areas of five samples were measured with a BET apparatus. Different samples have similar porosities and pore sizes. The average area was 0.61 ± 0.11 m^2/gm. The low surface areas rule out the possibility of a significant contribution of smaller pores to the measured porosity. A typical mercury porosimeter scan is shown in Fig. 1. Most of the penetration occurred at pressures corresponding to pore diameters of 1.1 to 0.6 μm. From the maximum penetration volume, the relative porosity was determined to be 0.45 ± 0.02.

The porous alumina with a smaller average pore diameter was prepared by isostatically pressing 0.6 micron alumina (Alcoa A16-SG) at 240 MPa and firing for about one hour at 1000°C. This material was also characterized with mercury porosimetry, BET surface area measurements, and scanning electron microscopy. A typical porosimeter plot is also shown in Fig. 1. Alumina II had an average pore diameter of 0.14 ± 0.01 μm, a porosity of 0.42 ± 0.01, and a surface area of 5.4 ± 0.1 m^2/gm.

If a porous material is approximated as a series of parallel capillaries, its average pore diameter, d, can be estimated from the relation $d = 4\ \varepsilon/S(\varepsilon-1)\ \rho$, where S is the surface area per gram, ε is the relative porosity, and ρ is the density [15]. This method yielded $d = 1.2 \pm 0.2$ μm for Alumina I. Scanning electron microscope (SEM) pictures confirm that pore cross sections are of the order of 1 μm, but show the pores to have very irregular shapes. These deviations from ideality reduce experimental transmission probabilities below those predicted for a bundle of parallel capillaries [16].

For a straight cylindrical tube with a length-to-radius ratio of 100 or greater, the transmission probability is $(4/3)(d/\ell)$ [17]. For a porous barrier, this becomes $(1/\tau)(4/3)(d/\ell)$, where τ, the tortuosity factor, is the ratio of transmission by Knudsen flow through ideal cylindrical orifices to transmission through a barrier of the same relative pore volume to surface area [18].

One apparatus was used for He and other gases, and a second was used for various high temperature vapors. The apparatus for gases is shown in Fig. 2. It consists of a gas bulb from which a gas can be leaked through a porous barrier. The rate of leakage is proportional to the transmission coefficient. The porous barrier is mounted on a smooth mullite tube and is held in place by a spring-loaded cap. This arrangement is designed to minimize escape other than through the porous barrier.

The rate of leakage from the gas bulb is the time derivative of the ideal gas law: $dn/dt = (V/RT_m)dP/dt$. Here V is the volume of the gas bulb and manifold, and T_m is the temperature of the gas in the manifold. The flow rate through the porous barrier is given by the Hertz-Knudsen-Langmuir equation, modified by W, the transmission probability. $J = (1/A)dn/dt = WP/(2\pi MRT)^{1/2}$, where M is molecular weight of He and T_b is the temperature of He in the barrier. Equating and integrating these two expressions for J gives $W = [(2\pi MRT)^{1/2}V/(A_pRT_m)]$ $(\Delta\ln P/\Delta t)$. Here A_p is the exposed area of the barrier fronted by pores (i.e., the exposed area multiplied by the porosity) and $\Delta\ln P/\Delta t$ is the rate of leakage from the bulb. This quantity was calculated from the output of the capacitance manometer.

The transmission properties of the high temperature vapors were determined from weight losses. A diagram of the apparatus is shown in Fig. 5. Alumina cells could not be used for LiF because it penetrated through at grain boundaries. Free energy calculations indicate that the reaction of NaF(g) and Al_2O_3 to form Na_2O and AlF_3 is not favorable under these conditions. The formation of cryolite, Na_3AlF_6, does have a free energy change of -674 kJ/mol at 1100°K:

$$12\ NaF(g) + Al_2O_3(s) = 2\ Na_3AlF_6(s) + 3\ Na_2O(s)$$

However, this indicates that cryolite would form only if the pressure for NaF exceeds 200 Pa. Since the pressure in the cell was never greater than 1 Pa, this reaction cannot occur. There was also no physical evidence of a reaction occurring to any large extent. After an experiment, the barrier gained at most about 1 mg compared to a total weight loss of 5 mg or more of NaF. The used barrier showed only alumina x-ray diffraction peaks, and the remaining sample showed only sodium fluoride peaks. Similar calculations and examinations indicated no evidence for reactions of LiF or NaCl vapors with alumina. A barrier was sectioned and studied by Auger spectroscopy after LiF runs. A small quantity of fluorine was detected at the inner surface, but fluorine was undetectable in the interior of the barrier.

Thick-walled boron nitride cells showed no evidence of reaction with the vapors studied, had good mechanical strength, and could be ground to give a good fit between the cell body and alumina barrier. As in the apparatus for gases, the system is designed to minimize escape via routes other than through the barrier.

Zinc and three alkali halide salts--sodium chloride, sodium fluoride, and lithium fluoride--were examined. Reagent grade chemicals were used for each. Solids will establish essentially equilibrium pressures in the source cell if their vaporization coefficients are large relative to the transmission probability through the barrier [1]. Zinc and the alkali halides have vaporization coefficients near unity [19], and barrier transmission coefficients were found to be $<10^{-2}$ in all measurements.

Exploratory heatings were made with the cell set at various heights in the furnace in order to find a position that gave no measurable condensation of vapor on the barrier. The cell, barrier, and material to be vaporized were initially weighed, loaded into the furnace, and rapidly brought to temperature. The temperature was maintained for a known time period (generally about 10 hours). The cell assembly was then rapidly cooled and weighed again. Several measurements were taken for each solid. Equilibrium fluxes were determined from weight-loss measurements on cells with orifices. These measurements were used for temperature calibrations and to give the flux impinging on the bottom of the barrier (J_o). Weight-loss measurements on cells with porous barrier lids gave the flux emerging from the barrier (J_e). The transmission probabilities are $W = J_e/J_o$. For NaCl, porous barriers like those used here shift the monomer-dimer equilibrium to yield only traces of dimer [14]. Similar behavior was found for NaF and LiF. Therefore, both orifice and porous barrier fluxes are expressed in terms of equivalent monomer units--$J_m + 2J_d$, where J_m is the monomer flux and J_d is the dimer flux.

The vacuum chamber used for these experiments was the Knudsen cell chamber of a Nuclide model HT-12-60 mass spectrometer. The temperature dependence of the effusing vapors could be determined using the mass spectrometer. In a mass spectrometer, ion intensity, I, and Temperature, T, are related to flux by $J = gIT/\sigma$ [20]. Here g is the machine constant and σ is the ionization cross section. Thus, when ion intensities are measured as a function of temperature, a plot of ln IT vs 1/T yields an enthalpy from the slope. For Knudsen effusion, this enthalpy is the enthalpy difference between the vapor and the condensed phase. If surface diffusion is the dominant path for vapor escape from a cell, the corresponding quantity calculated from the slope is the enthalpy difference between the transition state complex for surface diffusion and the condensed phase.

RESULTS AND DISCUSSION

Tortuosity factors have been found to have experimental values that range from 1 to 10. For the ∿1 mm thick alumina barrier with 1 μm pores, these limiting values of τ give predicted transmission probabilities of 1.3×10^{-3} to 1.3×10^{-4}. Four runs with He yielded $W = (6.51 \pm 0.86) \times 10^{-4}$ or $\tau = 2.0$. Other noncondensible gases gave similar results; for Ar, N_2, O_2, and CO_2, $\tau = 1.9$; for SO_2, $\tau = 2.0$; for NH_3, $\tau = 2.1$; for CH_4, $\tau = 2.4$. Average deviations for repeated measurements with the same gas were 15% except for CH_4 for which the average deviations were 23%. Gases for which surface diffusion is important should show larger transmission probabilities than that of He. Within the scatter in the data, transmission of each of these gases can be accounted for by Knudsen flow alone.

Table 1 shows that transmission coefficients for the three alkali halides through the alumina barrier with 1.2 μm pores, unlike those for the gases, exceeded the transmission coefficient for He by factors of 2 or more. The increase in transmission coefficients over that for He presumably must be due to contributions from surface diffusion.

Table 2 shows data obtained for zinc under three different sets of circumstances. Data reported under Ia are data collected under the same conditions as those reported for the alkali halides in Table 1. Data reported under heading Ib were made with the same apparatus and the same porous alumina, but later in time and with complete recalibrations of the apparatus for gas transmission and of that for studies of high temperature vapors. The He calibration is in reasonable agreement with that first obtained; 11 runs give an average transmission coefficient which is 24% higher than that obtained in the first set of runs. But the ratio of the zinc transmission coefficient to the He transmission coefficient was found to be 3.5 instead of 1.2.

We have been unable to identify the origin of this difference. It must be associated with a change in the high temperature apparatus or in the calibration. The most probable change which could account for the difference would be either a leak that increased the flux of zinc in the second apparatus or a difference in the temperature calibrations.

The runs reported under II were carried out with the alumina of smaller cross-sectional pore area in order to settle the question of whether or not zinc surface diffusion is significant in pores of the order of 0.1 to 1 μm cross section. In this barrier the He transmission was reduced by almost an order of magnitude, as expected from the change in average pore dimensions. Transmission for zinc was more than 18 times that for He. From the ratio of surface to Knudsen flux in the 0.14 μm barrier, 17, and the assumption that the ratio of surface to Knudsen fluxes should vary with 1/r the predicted surface flux contribution in 1.2 μm pores is found to be 2.0. It can be concluded, therefore, that surface diffusion makes an important contribution to the transmission of zinc vapor in alumina pores of 1 μm or less.

Below the melting points of LiF (Fig. 4) and NaCl (Fig. 5) the temperature dependences of the enhanced transmission through porous barriers were found to be essentially the same as the temperature dependences for effusion. Above the melting point of LiF the shapes of log intensity vs 1/T plots for effusion through an orifice were slightly reduced, as expected because the heat of vaporization of the liquid is less than that of the solid. In contrast, above the melting points, temperature dependence of the intensities measured through porous barriers increased and became erratic. Fig. 4 shows a discontinuity at the melting point. Another run made in an alumina cell which had not yet been penetrated by the LiF simply showed an increase in slope at the melting point, but then showed an upward discontinuity at a higher temperature.

If data had been collected only below the melting point, it might have been assumed that the rate-limiting process for vapor transport through the barrier is deposition of an adsorbed film on the inner barrier surface. But if that process were rate limiting, the temperature dependence of the transmission coefficient should remain the same as the temperature dependence of vaporization above the melting point as well as below. Thus, there is clearly a change in transport mechanism at the melting point.

It seems probable that the rate-limiting process below the melting point is surface diffusion in a film of <1 monolayer coverage and with the activated complex of the diffusional step being so loosely bound that its molecular properties approach those of the free vapor molecules. Above the melting point creep of a liquid-like film may become an additional path for partial penetration of the barrier. The distance to which the film penetrates before the alkali halide pressure gradient makes a liquid-like adsorbed film unstable would increase with temperature and would be sensitive to changes in the temperature gradient through the barrier. The rate-limiting step of surface transport thus would be diffusion in the same kind of submonolayer state that governs surface transport below the melting point but over distances that are shortened by penetration of the liquid-like film. Further studies in which the thickness of a barrier and the temperature gradient through it are deliberately varied are planned to test this line of reasoning.

We can conclude from our data that surface diffusion would not significantly influence effusion of the four solids studied here through long orifices of 0.1 mm or greater diameter in alumina or similar oxides (though grain boundary penetration is serious for LiF), but we do not know the effect of channel length. In the interpretation of porous barrier studies, surface diffusion and Knudsen flow have usually been interpreted as parallel and essentially independent processes. Such a model makes the relative importance of surface and Knudsen diffusion independent of channel length. Winterbottom and Hirth's model treat surface diffusion as directly dependent upon the local vapor flux. This model makes contribution of surface diffusion important only for very short channels. We suspect that the model which will reproduce the behavior of most vapors in effusion cells will be one that modifies the independent flux model of the porous barrier literature to account for the kinds of end effects that Winterbottom and Hirth evaluated.

ACKNOWLEDGMENT

Special thanks are due to Dr. David Meschi for his frequent advice in this study. Thanks are also due to the Lawrence Berkeley Laboratory ceramics shop for help in fabricating the porous barriers. This work was supported by the Division of Materials Science, Office of Basic Energy Science, U.S. Department of Energy under Contract Number DE-AC03-76SF00098.

REFERENCES

1. Paule, R.C., and Margrave, J.L., in The Characterization of High Temperature Vapors, Ed. by J.L. Margrave, John Wiley and Sons, New York, 1967, Chap. 6.
2. Cater, E.D., "The Effusion Method at Age 61: Current State of the Art," NBS Special Publication 561, 1979.
3. Ward, J.W., and Fraser, M.V., J. Chem. Phys. 50, 1877 (1969).
4. Huang, M., Meschi, D.J., and Searcy, A.W., unpublished work.
5. Winterbottom, W.L., and Hirth, J.P., J. Chem. Phys. 37, 784 (1962).
6. Winterbottom, W.L., J. Chem. Phys. 47, 3546 (1967).
7. Dunham, D.L., and Hirth, J.P., J. Chem. Phys. 49, 4650 (1968).
8. Ward, J.W., Bivins, R.L., and Fraser, M.V., J. Vac. Sci. Technol. 7, 206 (1970).
9. Ward, J.W., Fraser, M.V., and Bivins, R.L., J. Vac. Sci. Technol. 9, 1056 (1972).
10. Boyer, A.J., and Meadowcroft, T.R., Trans. Met. Soc. AIME 233, 388 (1965).
11. Grimley, R.T., Wagner, L.C., and Castle, P.M., J. Appl. Phys. 46, 4090 (1975).
12. Ash, R., Barrer, R.M., Clint, J.H., Dolphin, R.J., and Murray, C.L., Roy. Soc. (London) Phil. Trans. 275, 255 (1975).
13. Gilliland, E.R., Baddour, R.F., and Russell, J.L., AIChE Journal 4, 90 (1955).
14. P. Mohazzabi and A.W. Searcy, J. Chem. Phys. 65, 5037 (1977).
15. Satterfield, C.N., Mass Transfer in Heterogeneous Catalysis, MIT Press, Cambridge, Mass., p.41.

16. Nicholson, D., and Petropoulous, J.H., "Capillary Models for Porous Media with Special Reference to Gas Flow," in _Pore Structure and Properties of Porous Materials_, Proceedings of Internal Symposium RILEM/IUPAC, Prelim. Rpt. Part I, 1973, p.A-92.

17. Dushman, S., _Scientific Foundations of Vacuum Technique_, John Wiley and Sons, New York, 1955, p.98.

18. _Op. cit._, Satterfield, pp.35-41.

19. Searcy, A.W. "The Kinetics of Evaporation and Condensation Reactions," in _Chemical and Mechanical Behavior of Inorganic Materials_, Ed. by A.W. Searcy, D.V. Ragone, and U. Colombo, Wiley Interscience, New York, Chap. 6.

20. R.T. Grimby, in _The Characterization of High Temperature Vapors_, Ed. by J.L. Margrave, John Wiley and Sons, New York, 1967, Chap. 8.

Table I. Transmission probabilities for helium and alkali halide vapors. The porous alumina used had 1.2 ± 2 μm pores.

Gas or Vapor	Temp °K	No. of measure ments	Av. incident flux mole/cm^2-s	Av. trans- mitted flux mole/cm^2-s	Av. trans-* mission prob., W	W/W_{He}
He	295	4	-	-	$(6.51 \pm .86) \times 10^{-4}$	1.0
NaCl	1001	6	1.77×10^{-5}	3.00×10^{-8}	$(1.69 \pm .23) \times 10^{-3}$	2.6
NaF	1097	4	1.69×10^{-6}	6.61×10^{-9}	$(3.91 \pm .43) \times 10^{-3}$	6.0
LiF	1074	3	4.39×10^{-6}	3.49×10^{-8}	$(7.95 \pm .68) \times 10^{-3}$	12.2

*Uncertainties are standard deviations.

Table II. Transmission probabilities for helium and zinc vapors.

Gas or Vapor	Temp °K	No. of measure ments	Av.incident flux mole/cm^2-s	Av. trans-mitted flux mole/cm^2-s	Av. trans-mission prob.,* W	W/W$_{He}$
	Alumina Ia with 1.2 ± 0.2 μm pores					
He	295	4	-	-	$(6.5\pm0.8)\times10^{-4}$	1
Zn	630	5	7.62×10^{-6}	6.16×10^{-9}	$(8.09\pm1.45)\times10^{-4}$	1.2
	Alumina Ib with 1.2 ± 0.2 μm pores					
He	295	11	-	-	$(8.0\pm1.3)\times10^{-4}$	1
Zn	647	9	1.81×10^{-5}	5.08×10^{-8}	$2.81\pm0.67)\times10^{-3}$	3.5
	Alumina II with 0.14 ± 0.02 μm pores					
He	295	9	-	-	$(9.2\pm0.8)\times10^{-5}$	1
Zn	647	7	1.81×10^{-5}	3.04×10^{-8}	$(1.68\pm0.42)\times10^{-3}$	18

*Uncertainties are standard deviations.

FIGURES

Fig.1 Mercury porosimeter scans for both porous aluminas used.

Fig.2 Apparatus for measuring the transmission properties of helium.

Fig.3 Apparatus for measuring the transmission properties of high temperature vapors.

Fig.4 Plots of ln IT vs 1/T for LiF through a porous barrier and an orifice.

Fig.5 Plots of ln IT vs 1/T for NaCl through a porous barrier and an orifice.

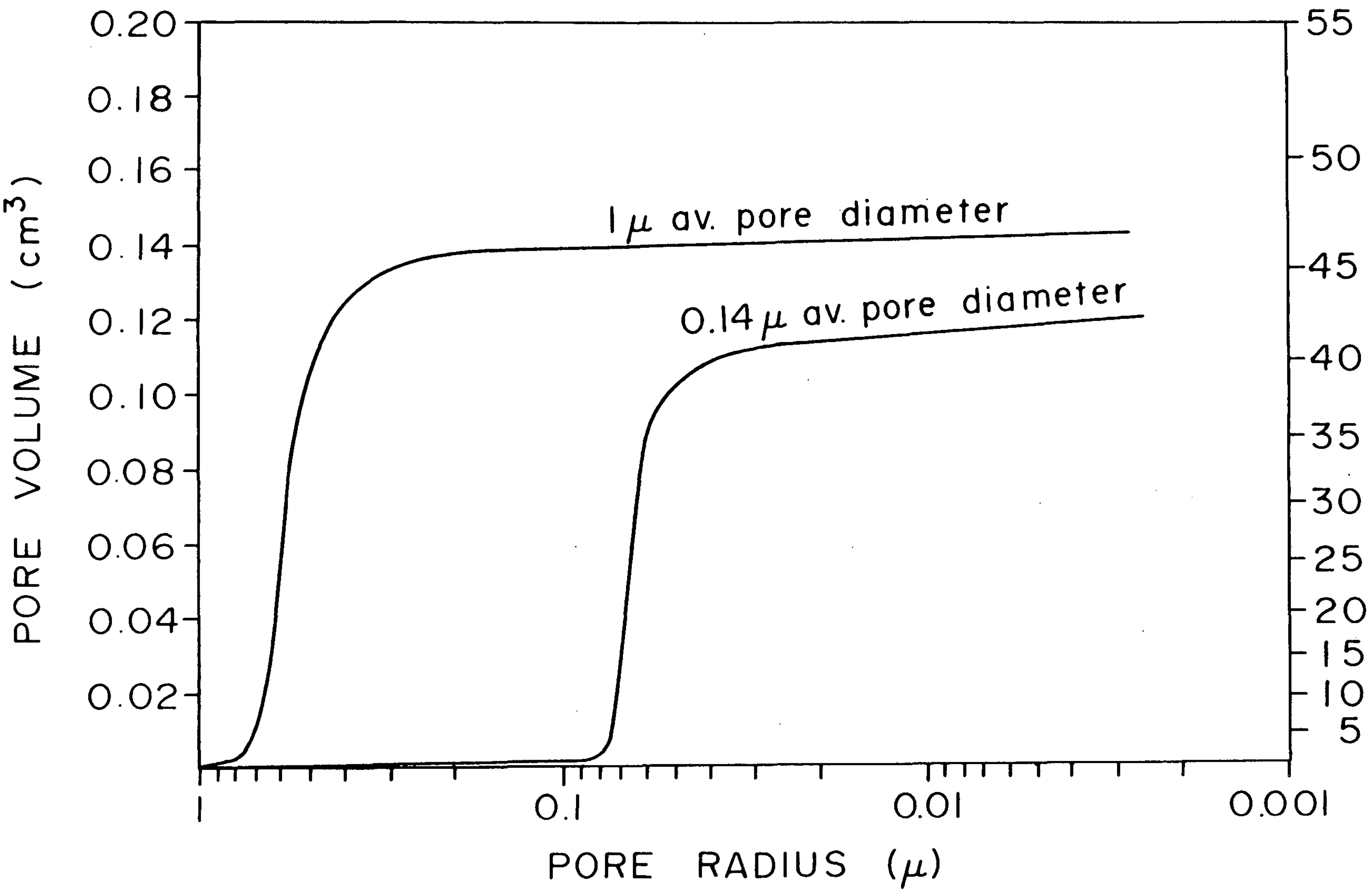

XBL 837-10814

Figure 1

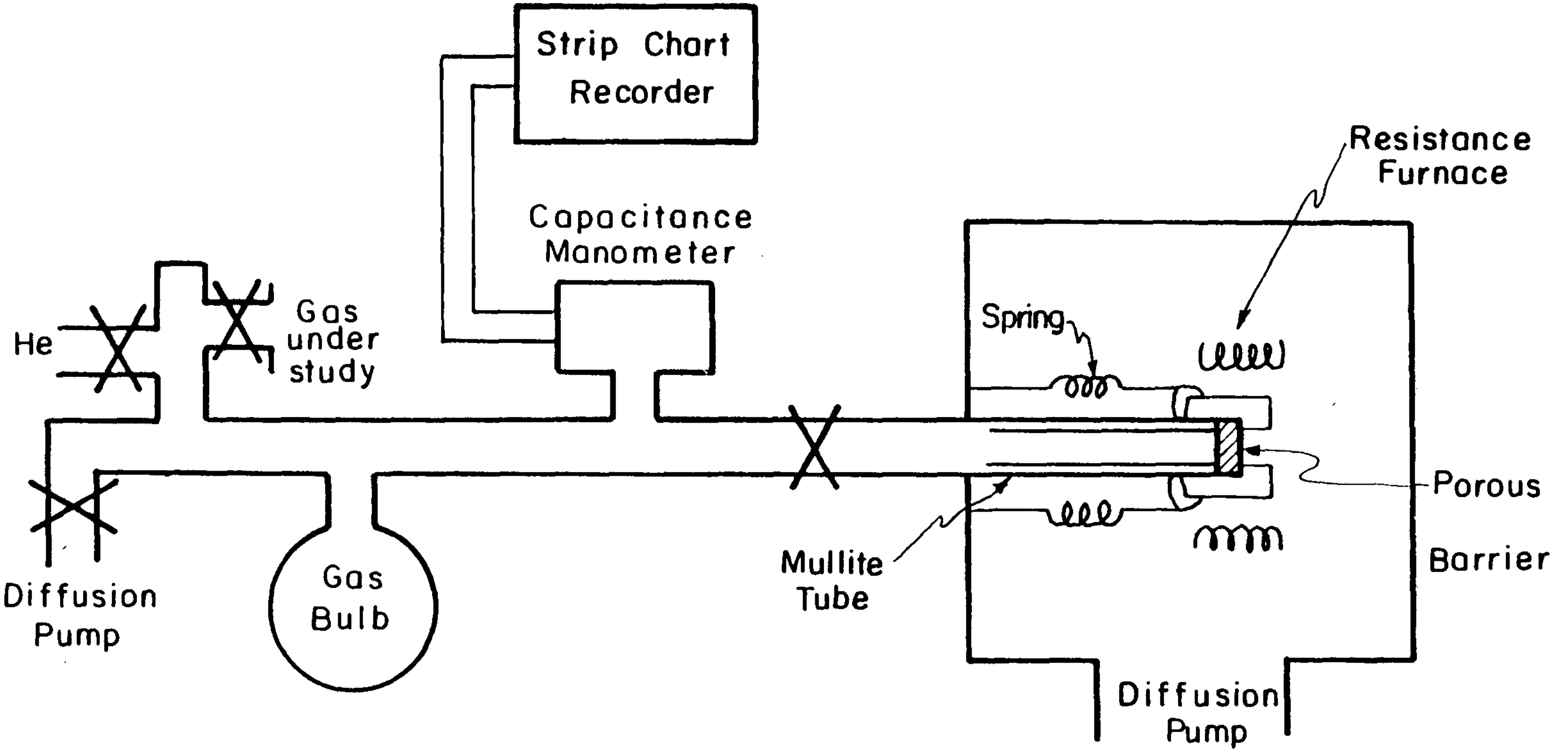

XBL816-6029

Figure 2

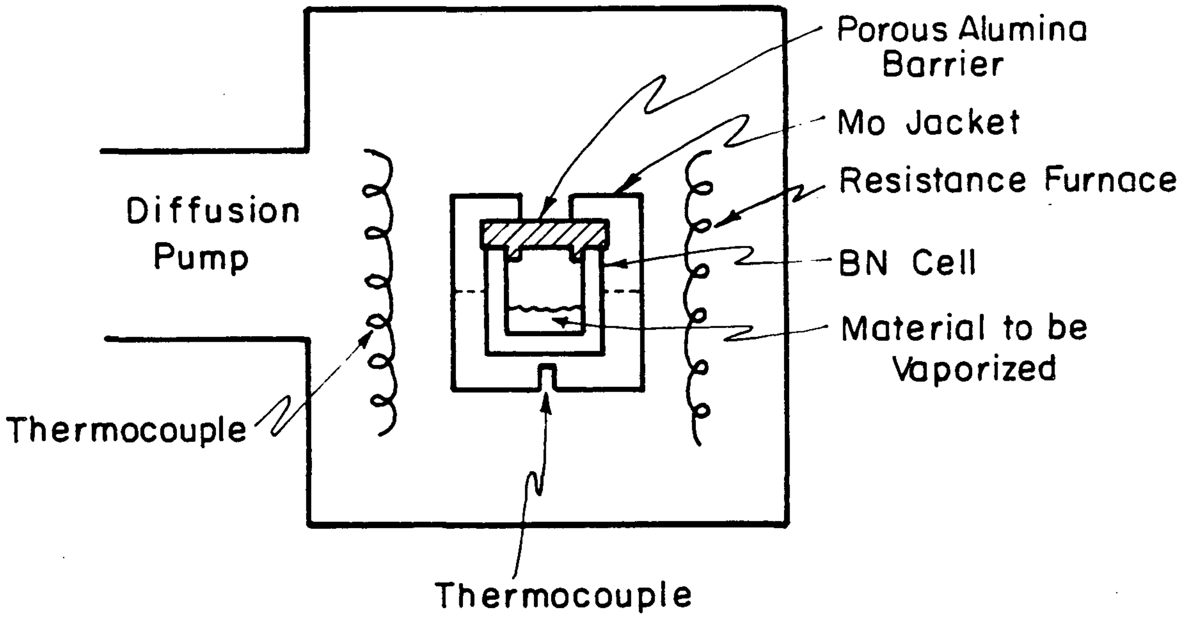

XBL 816-6030

Figure 3

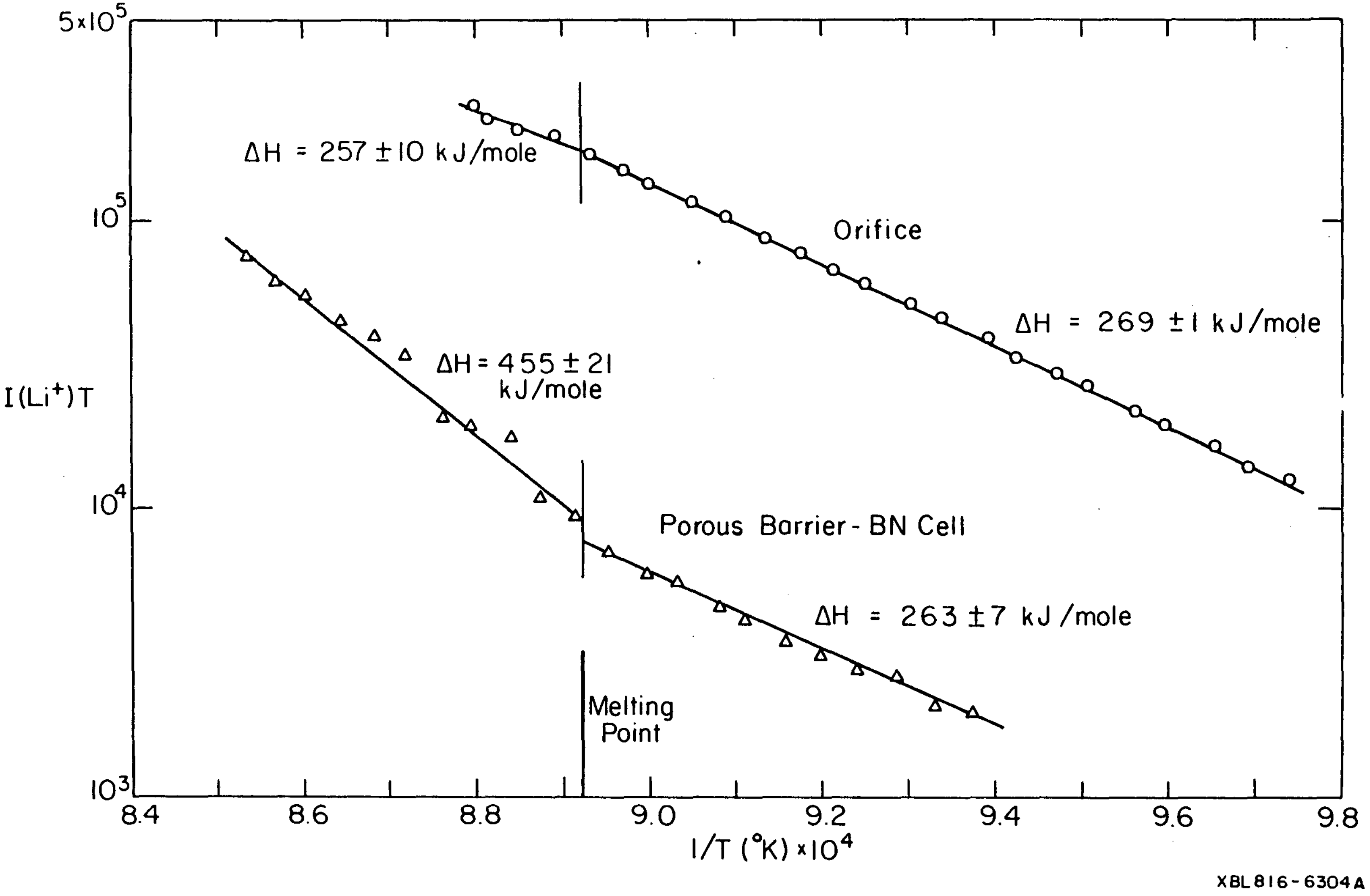
5×10⁵
10⁵
10⁴
10³
I(Li⁺)T
ΔH = 257 ± 10 kJ/mole
Orifice
ΔH = 269 ± 1 kJ/mole
ΔH = 455 ± 21 kJ/mole
Porous Barrier - BN Cell
ΔH = 263 ± 7 kJ/mole
Melting Point
8.4
8.6
8.8
9.0
9.2
9.4
9.6
9.8
1/T (°K) ×10⁴
XBL 816-6304 A

Figure 4

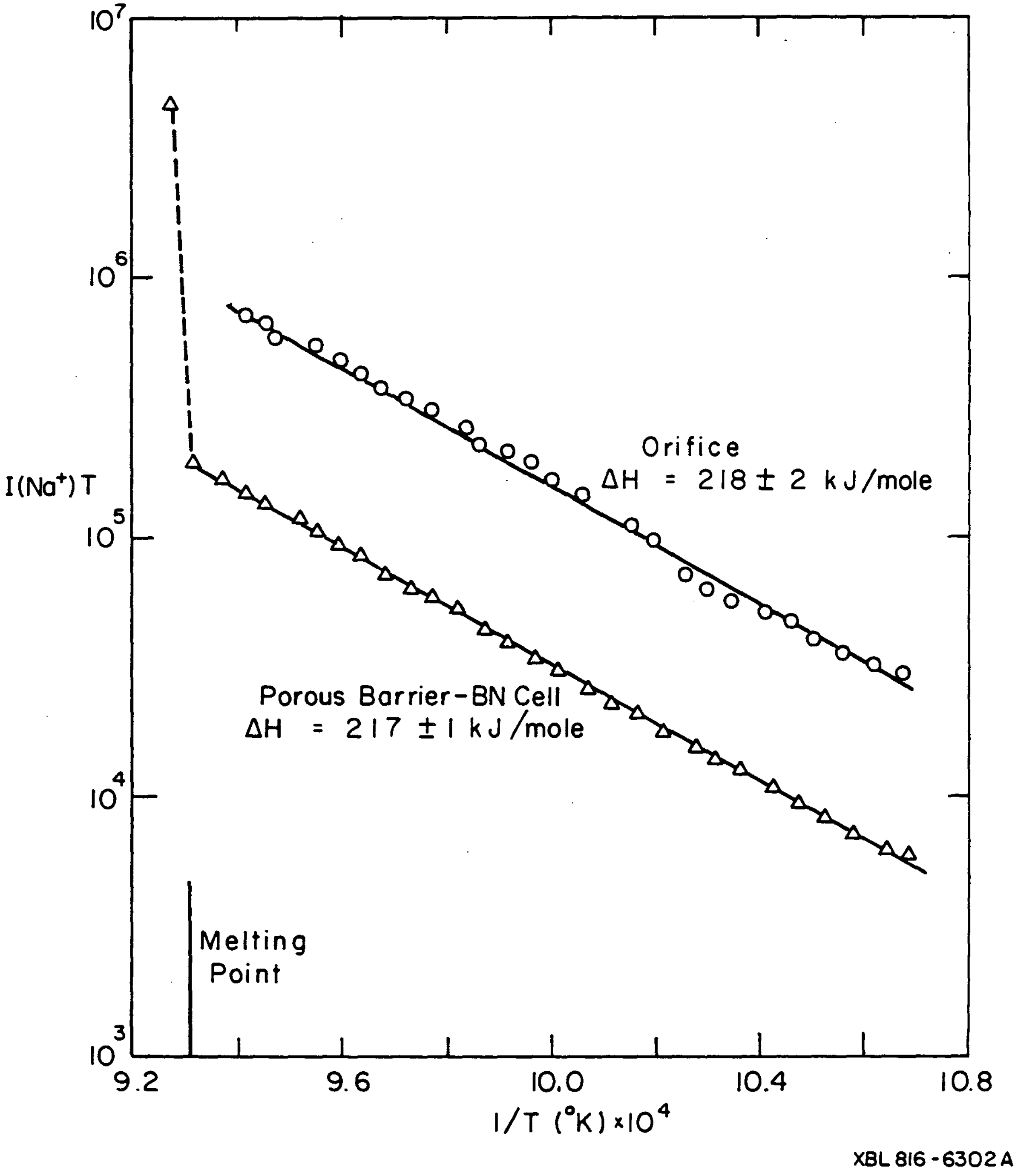
10^7
10^6
10^5
10^4
10^3
I(Na+)T
Orifice
ΔH = 218 ± 2 kJ/mole
Porous Barrier-BN Cell
ΔH = 217 ± 1 kJ/mole
Melting Point
9.2
9.6
10.0
10.4
10.8
1/T (°K) ×10^4
XBL 816-6302 A

Figure 5

TECHNICAL INFORMATION DEPARTMENT
LAWRENCE BERKELEY LABORATORY
UNIVERSITY OF CALIFORNIA
BERKELEY, CALIFORNIA 94720